Comprehensive Analysis of Principal Slot Harmonics as Reliable Indicators for Early Detection of Inter-turn Faults in Induction Motors of Deep-Well Submersible Pumps

Jorge Bonet-Jara, Joan Pons-Llinares, *Member, IEEE* and Konstantinos N. Gyftakis, *Senior Member, IEEE*

***Abstract*—Early detection of inter-turn faults is one of the most important issues in electrical machines, as the fault severity evolves very fast to a catastrophic failure due to the high thermal stress. However, as this paper shows, in submersible induction motors for deep-well pumps, it evolves slower. These motors are highly water-cooled, which significantly reduces the thermal stress caused by the fault, increasing the possibility of an early detection. Among fault detection methods, only those based on line current/voltage measurements can be used, as motors are at great depths. This article investigates the Principal Slot Harmonics as reliable indicators for early detection of inter-turn faults in this application. To this end, a comprehensive analysis is conducted using finite element analysis where the behavior of these harmonics is studied under different fault severities, both alone and coexisting with other asymmetries such as unbalanced voltages, eccentricity or rotor faults. The findings are used to develop a reliable diagnostic scheme based on the monitoring of the most fault-sensitive harmonics along with the voltage and current unbalance indexes. Finally, the scheme is applied, for the first time, in the context of a continuous monitoring of a 230 HP induction motor showing its efficacy.**

***Index Terms*—Condition monitoring, inter-turn faults, induction motors, fault diagnosis, MCSA, finite-element analysis, pumps**

I. Introduction

DEEP well water pumps are starting to play an essential role in human's water supply, since superficial aquifers are drying due to climate change [1]. These pumps are normally driven by water-cooled squirrel cage submersible induction motors [2]. Therefore, monitoring the condition of this element is a key aspect to avoid catastrophic failures and unexpected shutdowns, which is quite a sensitive issue in this industry, due to the cost of replacement (motors are in wells of up to 500 m in depth) and the fact of leaving a part of the population without water supply.

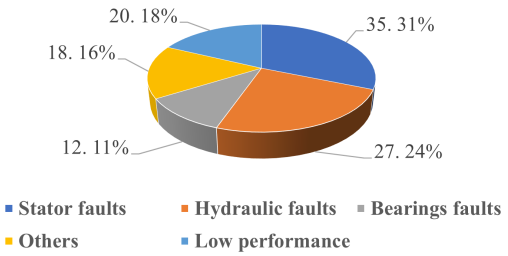

Fig. 1. Distribution of reasons for pump replacement in a Spanish water company.

Data provided by a Spanish water company on 20 water pumping facilities over the last three decades show that the main reason for pump replacement is found in stator faults (Fig. 1). A recent study has shown that end-rings of deep-well motors wear quite often [3]. This is due to the particular characteristics of their rotor cage (copper liquid soldering glues together bars and a set of die-cut thin end-ring sheets), the internal water cooling system and the high rotational speed (due to one pole pairs design). The particles detached from the end-ring wear is a possible trigger mechanism for the degradation of insulation in the stator coils.

Another particular characteristic of these machines is their cooling system which is done both externally (by forcing the water to flow through the motor surface) and internally (by pre-filling the motor with a mixture of water and glycol). Thus, stator windings are subjected to a less thermal stress than in conventional surface motors, which delays the propagation of an inter-turn fault to a phase-to-phase or phase-to-ground short-circuit. Therefore, there is a higher probability of detecting the failure at an early stage.

In the field of on-line diagnostics, several methods have been proposed to detect inter-turn faults. However, some of them are unfeasible in their application to deep-well pumps. Flux [4]–[8] and vibration [9]–[11] methods require installing a sensor at or near the surface of the motor. This is a big challenge in deep-well motors, since the sensor must be able to withstand the impedance of an up to 500 m cable, be waterproof, be fixed in the smooth outer surface of the

This work was supported by the Universitat Politecnica de Valencia and the Spanish Ministry of Science, Innovation and Universities [FPU19/02698].

Jorge Bonet-Jara and Joan Pons-Llinares are with the Instituto Tecnológico de la Energía, Universitat Politècnica de València, C/Camino de Vera s/n, 46022, València, Spain (e-mail: jorboja@die.upv.es; jpons@die.upv.es).

Konstantinos N. Gyftakis is with the School of Electrical & Computer Engineering, Technical University of Crete, Akrotiri Campus, 731 00, Chania, Greece (e-mail: k.n.gyftakis@ieee.org).

motor and survive the descent to the aquifer through a narrow borehole. In turn, methods that use the zero-sequence current or require access to the neutral point [12]–[14], cannot be applied, as coil end-connections are done internally in these motors, and therefore, phase magnitudes are not accessible. Thus, the only feasible solution in this application is to use methods based on line current/voltage measurements, as they are available at the motor control cabinet. In this regard, different approaches have been followed over the last two decades. Motor Current Signature Analysis (MCSA) has been proposed to monitor the amplitude of the third harmonic or the Principal Slot Harmonics (PSHs) [15]–[19], as well as instantaneous active/reactive power signature analysis to monitor the second harmonic [20]. The theory of symmetrical components has also been used based on the relationship between the asymmetry created by the stator fault and the negative sequence component [21], [22]. In recent years, advances have been made regarding model-based and artificial intelligence techniques [23]–[26].

Concluding, existing methods for inter-turn fault detection based on flux and vibration [4]–[11] are difficult to be applied in deep-well motors, since these motors are submerged at great depths (up to 500 m), while methods that use the zero-sequence current or neutral point cannot be applied, as phase magnitudes are not accessible [12]–[14]. Previous conclusions of line magnitude methods [15]–[26] have been deduced for conventional induction motors, and they are not necessarily valid in this specific context. Moreover, most of these line magnitude based works do not analyze in great detail the sensitivity and reliability of the proposed indicators in the presence of other asymmetries (in the most complete works the robustness of the method is studied only under eccentricity and voltage unbalance [20] and under broken bars and voltage unbalance [24]). In addition, these diagnostic schemes have not gone beyond laboratory tests where low power motors are used (with the exception of [16], [17] and [20]). All this calls into question the applicability of these methods to real and large industrial motors.

This is the first paper to investigate how the special characteristics of deep well induction motors (e.g., double water cooling, low number of turns per slot, two poles and even number of rotor bars) together with their operating conditions (long steady state under constant load) act as game changers in terms of inter-turn fault detection through PSHs, making them much more reliable indicators than what is shown in other papers of conventional motors. The paper proves that in deep-well motors there is always a set of PSHs that are nearly absent in the healthy machine, and highly increase when the inter-turn short-circuit takes place, deducing a formula to determine them (highly improved reliability with respect to using PSHs present in healthy state, as previous methods). Moreover, it is proven that an incipient stator fault in deep-well motors does not cause a destructive current (it can be even lower than rated current) and that the double water cooling system of these motors prevents from a fast insulation degradation (fault detected at an early stage before becomes catastrophic). These characteristics, together with a very sensitive indicator, enables an early short-circuit detection. Apart from these very sensitive PSHs, two more indexes are proposed in order to discriminate inter-turn short-circuits from other asymmetries: Voltage Unbalance Index (VUI) and Current Unbalance Index (CUI). Theoretical findings are validated using up to 65 different simulations obtained through Finite Elements Analysis (FEA) on a 22 kW deep-well induction motor (high precision thanks to complete manufacturer data), and a detailed analysis is presented on the sensitivity and reliability of these harmonics under inter-turn faults, both alone and coexisting with different levels of voltage unbalance, rotor asymmetry and eccentricity. Finally, an original diagnostic scheme is presented to detect inter-turn faults through the use of PSHs, VUI and CUI, obtained only with line magnitudes, generating extremely sensitive indicators, even for early stages where other PSHs fail. Its efficacy is proven for the first time in the context of a continuous monitoring of a deep-well induction motor (230 HP) operating in a pumping station, where data has been collected every six hours for nearly a year.

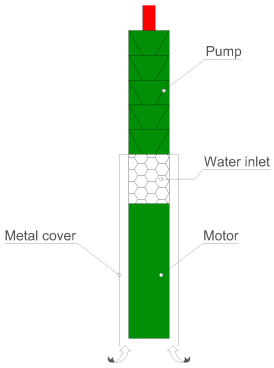

Fig. 2. Schematic of the motor-pump assembly.

II. Special features of induction motors in deep-well pumps

The motor and the pump work submerged in the aquifer, with shafts directly coupled and in vertical position; from bottom to top: motor - water inlet - pump - pipe. The motor frame is smooth and without heat sinks. Cooling is achieved in two ways: by pre-filling the motor with a mixture of water and glycol (internal cooling) and by placing a metal cover to force water flow between the cover and the motor surface before entering the pump (external cooling) [3]. Figure 2 shows the schematic of the motor-pump assembly.

As for the motor design and operating characteristics, two poles are used to achieve high power and speed with a small diameter (reducing excavation costs). Usually, an even number of rotor bars is used to avoid the unbalanced magnetic pull. Motors are fed with frequency converters or soft starters, sometimes working continuously for long periods of time and without significant load or speed variations, as water is usually pumped to a tank.

These characteristics make the motors particularly suitable for early detection of inter-turn faults via PSHs through an FFT steady-state analysis. First, because stator windings are subjected to less thermal stress than surface motors (they are

doubly water-cooled, with a very constant ambient temperature of around 15°C in the aquifer), which can retard the time between the inter-turn fault occurs and the moment it propagates to a catastrophic failure. Secondly, due to the small diameter of these motors, slots are smaller, and the number of conductors per slot (and phase) is smaller too. Hence, the small number of turns of an early-stage short-circuit represents a higher percentage (with respect to the total number of phase turns) than in conventional motors, thereby becoming a more noticeable fault. Third, due to rotor characteristics (two poles with an even number of rotor bars), motors are PSHs producers [27]. These harmonics are known to be correlated with the stator inter-turn fault [16]. Fourth, because, there are no false positives due to load variations, as this is practically constant, and therefore, PSHs amplitudes do not significantly change under normal operation. Finally, because due to the speed is also practically constant, together with the fact that these motors can run continuously for long periods of time, ideal conditions exist to apply a steady-state analysis using the FFT, and the best results can be obtained from it.

The PSHs frequencies are given by the Rotor Slot Harmonics formula [28] when $k = 1$:

$$f_{RSH} = \left[k\frac{R}{p}(1-s) \pm \nu \right] f_0 \tag{1}$$

where $k \in \mathbb{N}$, p is the number of pole pairs, s the slip, ν the orders of the time harmonics present in the stator current $1, 3, 5 \ldots$, f_0 the fundamental supply frequency and R the number of rotor bars.

A PSH appears in the line current if the relative order of its associated spatial flux harmonic wave is an odd number non-multiple of three. In a perfectly symmetrical machine, this relative order is given by $h_{rot} = R/p \pm h_{st}$, where h_{st} is the relative order of the spatial harmonic through which the time harmonic νf_0 interacts with the rotor system. Taking this into account, it can be proven that the two PSHs with the lowest $|\nu|$ absent in the line current are (with $n \in \mathbb{N}$):

- For $R/p = 6n - 4$: PSH($\nu = -5, 1$).
- For $R/p = 6n - 2$: PSH($\nu = -1, 5$).
- For $R/p = 6n$: PSH($\nu = -3, 3$).

In real machines, where inherent asymmetries exist, all these harmonics are present in the line current, although with very small amplitudes. Thus, as their existence is directly related to the level of asymmetry, and their amplitudes are practically zero in the healthy machine, they will be the most sensitive PSHs to an inter-turn fault. Therefore, these harmonics are the key to a real solution for the difficult task of detecting intern-turn short-circuits.

III. Finite-element analysis

The purpose of this section is to perform a comprehensive analysis on the sensitivity and reliability of PSHs as indicators for inter-turn fault detection. To this end, a FEA approach is used, since the idiosyncrasy of the motors under study does not allow to perform proper tests in an academic laboratory. This is because in order to obtain valid and comparable conclusions, a deep-well motor should be used, as their special characteristics

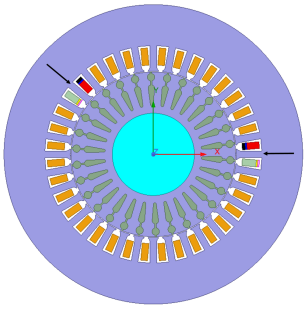

Fig. 3. Cross section of the motor with the coils divided in groups (arrows) to create the inter-turn fault with 6.06% of shorted turns.

affect the behavior of the motor under the short-circuit and its diagnosis through PSHs. To replicate industrial conditions, the deep-well motor should be tested under load, for which it would require a well, a pump coupled to the motor, a crane to put the motor inside the well and a system of pipelines and valves to regulate the load: if it is tested surrounded by air, it would over-heat very easily. However, these elements are difficult to be found in an academic laboratory. Therefore, as the laboratory test is not an option with this type of motors, a finite element analysis approach is followed, since it allows to perform very realistic and accurate short-circuit tests, with the motor in load, without compromising the integrity of the motor, while allowing an easy combination of the fault with different asymmetries of different severity.

In this regard, a submersible induction motor (22 kW, $p = 1$, 30 rotor bars, 230 V Δ, 65.6 A, 2900 rpm) has been modeled using a commercial FEA software. To ensure accuracy, complete geometry and B-H characteristic are provided by the manufacturer. The inter-turn fault is created in phase A, following the approach described in [29]. In this approach, the coils inside two adjacent stator slots are divided into groups. For example, Fig. 3 shows the cross section of the motor for the last of the inter-turn faults considered, where the coils that are placed in slots 1-16 and 2-15 have been divided into three groups (each of the groups is represented by a color and has a certain number of conductors). The short-circuit is then created between the middle groups of the adjacent slots, which consist of a single wire (a one-turn coil), through a contact resistance of 0.1 Ω. The fault severity is handled by modifying the number of conductors in the rest of the groups. Using this approach, the severity of the first four fault states is 1.52 %, 3.03 %, 4.55 % and 6.06 % of shorted turns.

Table I shows, for each fault state (column 1), the line A, phase A, short-circuit and contact resistance currents (columns 2-5); being the last two the currents through the short-circuited coils and the contact resistance respectively. The ratios of these magnitudes with respect to the healthy current (65.57 or 37.87 A) are shown in columns 6-9. Finally, column 10 shows the line Current Unbalance Index (CUI): maximum deviation in RMS value of any of the three line currents with respect to the mean value of their RMS values divided by this mean value.

It can be seen that in this machine the short-circuit currents are less severe than in previous studies for other types of machines and same severity level, where $I_{sc}/I_{A,h}$ ratio is up

TABLE I
RMS VALUES AND FAULT INDEXES OF THE CURRENTS IN THE MACHINE WITHOUT EXTRA ASYMMETRIES.

	$I_{l,A}(A)$	$I_A(A)$	$I_{sc}(A)$	$I_{cr}(A)$	$I_{l,A}/I_{l,A,h}(\%)$	$I_A/I_{A,h}(\%)$	$I_{sc}/I_{A,h}(\%)$	$I_{cr}/I_{A,h}(\%)$	$CUI(\%)$
H	65.57	37.87	-	-	-	-	-	-	-
F1 (1.52%)	65.92	38.39	17.60	35.30	100.52%	101.38%	46.48%	93.22%	0.43%
F2 (3.03%)	66.96	39.81	33.77	66.33	102.12%	105.14%	89.17%	175.18%	1.66%
F3 (4.55%)	68.65	42.07	54.00	92.87	104.69%	111.11%	142.61%	245.25%	3.61%
F4 (6.06%)	71.09	45.26	76.66	120.09	108.41%	119.53%	202.44%	317.14%	6.18%

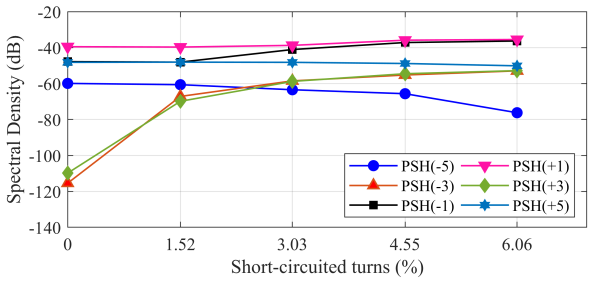

Fig. 4. Amplitude of PSHs for each fault state considered.

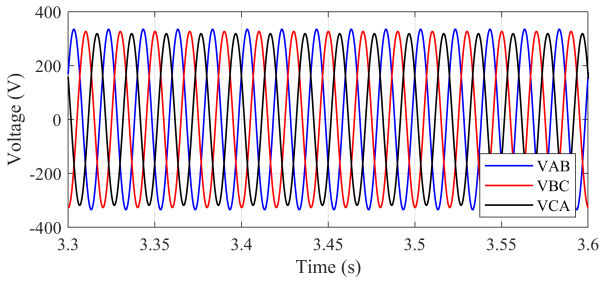

Fig. 5. Line voltages for a voltage unbalance index of 2.5%.

to two times higher [8], [29]. In fact, the first two fault states originate a short-circuit current that is even lower than the rated phase current (46.48% and 89.17%). This suggests that the fault can be detected at an early stage before it becomes catastrophic. However, the current flowing through the contact resistance is almost equal to the rated phase current in the first fault state and 1.75 times higher in the second. This leads to the formation of a heat source in a very small area that will eventually deteriorate the insulation and propagate the fault to the next stages. Therefore, protective measures should be taken as soon as possible. In this regard, none of the cases considered would activate the overcurrent protections, since the line current in the most severe case only exceeds the rated line current by 8.41%.

Thanks to the theoretical analysis of the previous section, it can be deduced that, for this motor combination of R and p, the PSHs($\pm$3) are absent in the line current spectrum of the healthy machine. When the asymmetry is introduced via the inter-turn fault, these harmonics should become the most sensitive to it, since any change in the amplitudes of the state of the art indicators (PSH(+1) or PSH(-1)) is masked due to their already high amplitude in the healthy state. This is exactly what can be seen in Figure 4, which shows, for each fault state considered, the amplitudes of the PSHs in the line A current spectrum (in dB with respect to the fundamental component; noise floor around -110 dB; similar conclusions for lines B and C). From the simulations results, it can be concluded that an extremely sensitive indicator for inter-turn faults has been found, even for early stages where other PSHs fail: (PSHs($\pm$3) show an extremely high change of 40 dB from healthy to only 1.52% of shorted turns, and a very high 10 dB change from 1.52% to 3.03%. Next, the reliability of using these PSHs as indicators for inter-turn faults is analyzed under the presence of different asymmetries with different severity levels.

A. Machine with unbalanced supply

Using NEMA MG 1-2016 definition, four levels of Voltage Unbalance Index (VUI) have been considered: 0.25%, 0.5%, 1% and 2.5%. According to this norm, with the first three levels of VUI a motor shall operate successfully, while with the last level it should be derated. Figure 5 shows the line voltages for a VUI of 2.5%. Figures 6a, 6b, 6c show, respectively, the amplitudes of the PSH(-3) and PSH(+3) in the line A current spectrum, and the CUI, for each inter-turn fault considered (x-axis), and each level of VUI (different colors).

PSH(+3) presents a strictly increasing behavior at all levels of VUI. Since the asymmetry introduced by the voltage unbalance gives rise to the PSHs($\pm$3) in the healthy machine (0% of short-circuited turns), amplitude difference with first fault stage (1.52 %) is bigger in the case without voltage unbalance (0 % VUI). Despite this, sensitivity to detect the fault is very high, especially in those stages in which the short-circuit current is still not catastrophic (1.52% and 3.03% shorted turns): at VUI not considered dangerous for the motor (VUI from 0.25 to 1%), from healthy to 1.52%, PSH(+3) amplitude increases between 1.5 dB and 5.3 dB, while from 1.52% to 3.03% increases between 4 dB and 8 dB.

On the other hand, PSH(-3) only presents a strictly increasing behavior for the first level of VUI. In the next two levels of VUI, this behavior starts at the first stage of inter-turn fault, while in the last level of VUI there is no clear trend. Yet, the sensitivity to the fault between the two non-catastrophic inter-turn faults for the three first levels of VUI is higher than in the PSH(+3) (changes going from 7 dB to 10 dB). Similar results are observed in line B. In line C, no strictly increasing behavior is observed for PSH(+3) and only from the first stage onwards for the PSH(-3).

Concluding, depicting the evolutions of the amplitudes of both PSHs(+3,-3) in the three currents, there are two evolutions out of six that maintain a strictly increasing behavior with the fault severity for all levels of VUI (PSH(+3) in lines A and B),

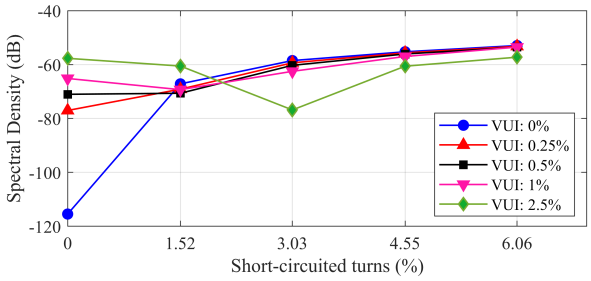

(a)

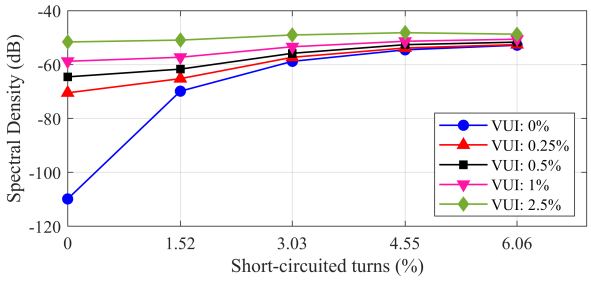

(b)

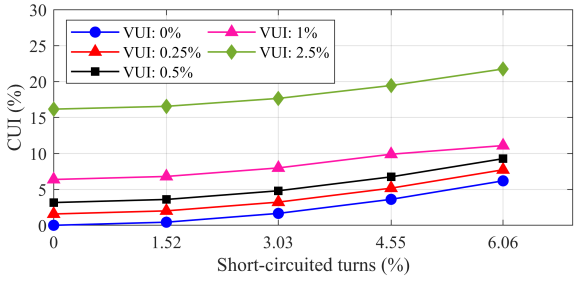

(c)

Fig. 6. Amplitude of PSH(-3) (a) and PSH(+3) (b) in line A spectrum, and CUI (c), for each inter-turn fault and each level of VUI.

enabling the fault detection at an early and non-catastrophic stage. As for the CUI, it strictly increases at all levels of VUI with practically the same change between fault stages.

However, it should be noted that the increase in the VUI for a same inter-turn fault creates significant variations in the PSH($\pm$3). For the healthy machine and the first two levels of intern-turn fault, this increase has a monotonic behavior, and consequently, can lead to a false positive. The same is observed for the CUI, but in this case, for all fault stages. Yet, if the VUI is also monitored it can be easily determined if the changes in these three indicators are due to a voltage unbalance or an inter-turn fault.

B. Machine with eccentricity

Combining static eccentricity (SE) with dynamic eccentricity (DE), four levels of eccentricity have been considered: SE:5% + DE:5%, SE:10% + DE:10%, SE:20% + DE:20% and SE:30% + DE:30%. According to [30], the first case is within the permissible levels for inherent eccentricity, the second and third cases are considered unacceptable and the last case is a serious problem requiring motor decommissioning. Figure 7 shows the amplitude of the Mixed Eccentricity Harmonics

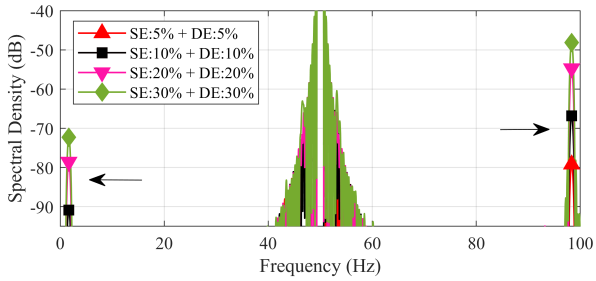

Fig. 7. Mixed Eccentricity Harmonics for each level of eccentricity in the machine without inter-turn fault.

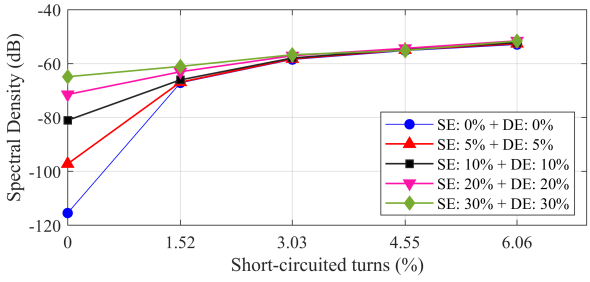

(a)

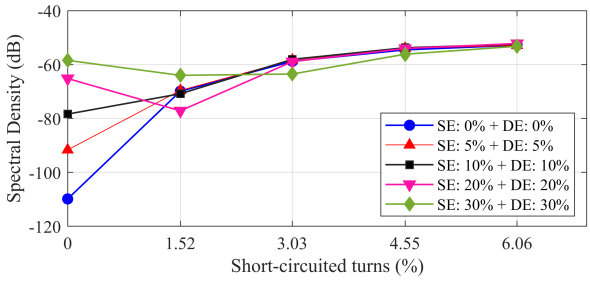

(b)

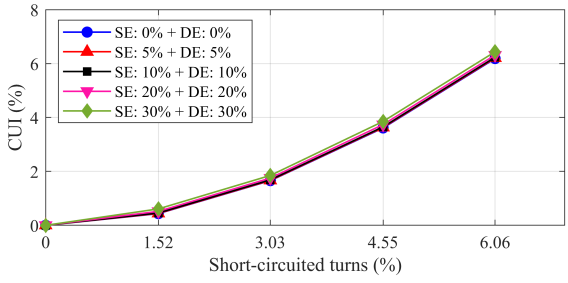

(c)

Fig. 8. Amplitude of PSH(-3) (a) and PSH(+3) (b) in line A spectrum, and CUI (c), for each inter-turn fault and each level of eccentricity.

(MEH) due to each eccentricity level for the machine without inter-turn fault. Figures 8a, 8b, 8c show, respectively, the amplitudes of the PSH(-3) and PSH(+3) in the line A current spectrum, and the CUI, for each inter-turn fault considered (x-axis), and each level of eccentricity (different colors).

PSH(-3) presents a strictly increasing behavior with respect to the short-circuit severity, for all levels of eccentricity. From healthy to 1.52%, PSH(-3) amplitude increases between 4 dB and 31 dB, while from 1.52% to 3.03% it increases between

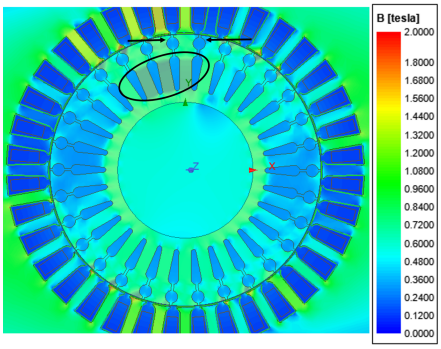

Fig. 9. Magnetic flux density distribution for the case of 2 broken bars (arrows) without inter-turn fault.

4 dB and 9 dB.

In the case of the PSH(+3), the strictly increasing behavior is lost at the first stages for the two most severe levels of eccentricity, but maintains an overall better sensitivity to the fault severity than the PSH(-3). Similar results can be observed in the line B and C, although in the latter, the strictly increasing behavior of PSH(-3) is already lost for the first fault in the second, third and four level of eccentricity. Thus, in the presence of the asymmetry caused by the eccentricity, it is also important to monitor both harmonics in at least two of the three currents. As for the CUI, it strictly increases in all levels of eccentricity with very small differences between them.

It should be noted that an inter-turn fault monitoring, based solely on tracking PSHs, could lead to a false positive in a healthy motor (and a false increase of the fault severity on the machine with 1.52% shorted turns), as the increase in eccentricity causes a monotonic increase in PSHs($\pm$3). Nevertheless, in this case, the CUI can be used to rapidly discriminate whether the increase in PSHs($\pm$3) is due to an eccentricity fault or an inter-turn fault, as this parameter strictly increases with the shorted-turns, but is insensitive to eccentricity changes (see Fig. 8c).

C. Machine with rotor asymmetries

Analyzing the impact of rotor asymmetries is very important in deep-well motors since, as explained in the introduction, their end-rings wear quite often [3]. By modifying the conductivity of the bars, four levels of rotor asymmetry have been defined: inherent asymmetry (IA), incipient fault (IF), 1 broken bar (1BB) and 2 broken bars (2BB). Figure 9 shows the magnetic flux density distribution for the case of 2 broken bars without inter-turn fault. As can be seen, there is an area (ellipse) near the broken bars (arrows) where an increase of the magnetic flux density exists, causing the magnetic asymmetry. This asymmetry is reflected in the line current spectrum through the Lower Sideband Harmonic (LSH), which is normally the harmonic used to diagnose this fault. In the absence of false indications [31], it is well established that amplitudes below -50 dB correspond to inherent asymmetry, between -50 dB and -40 dB to an incipient fault, -40 to -35 dB to a broken bar and above -35 dB to multiple broken bars. Figure 10 shows the amplitude of the LSH due to each

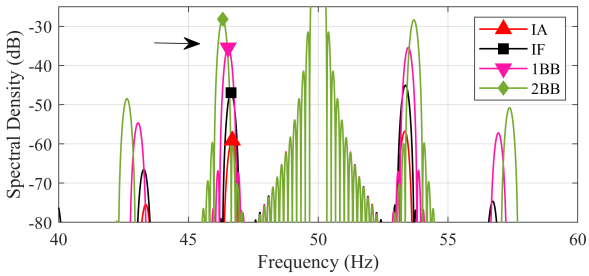

Fig. 10. LSH for each level of rotor asymmetry in the machine without inter-turn fault.

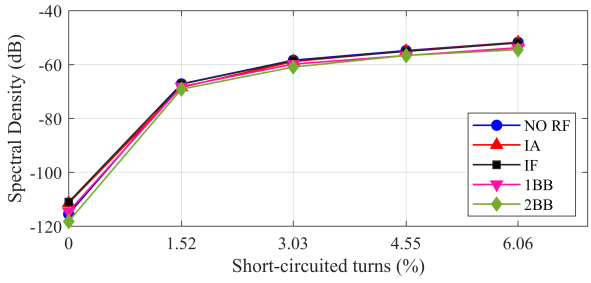

(a)

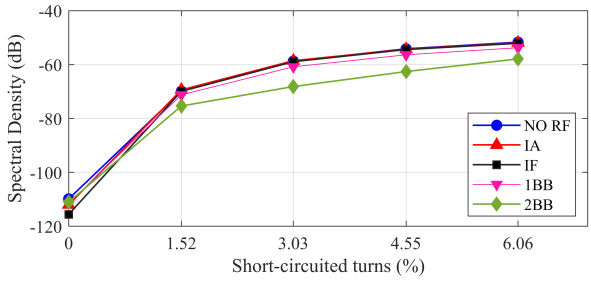

(b)

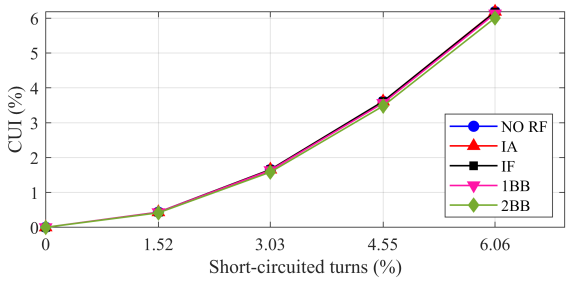

(c)

Fig. 11. Amplitude of PSH(-3) (a) and PSH(+3) (b) in line A spectrum and CUI (c) for each inter-turn fault and each level of rotor fault.

rotor fault for the machine without inter-turn fault. Figures 11a, 11b, 11c show, respectively, the amplitudes of the PSH(-3) and PSH(+3) in the line A current spectrum, and the CUI, for each inter-turn fault considered (x-axis), and each level of rotor fault (different colors).

In this case, both harmonics present a strictly increasing behavior for all levels of rotor fault considered. Moreover, PSH(-3) is practically insensitive to the rotor fault severity, while PSH(+3) presents sensitivity only to the most severe

case (2 broken bars). The same behavior is observed in line B, while it differs in line C as in the two previous asymmetries. As for the CUI, it is also insensitive to the rotor fault and shows a strictly increasing behavior for all levels considered.

Unlike the other two asymmetries studied, in this case it is not possible to get a false positive since there is one harmonic that is totally insensitive to the fault. Anyway, the CUI can always be used to discriminate, since it changes with short-circuited turns, but is not affected by rotor asymmetry.

IV. Monitoring method for a reliable detection

Thanks to the theoretical analysis in Section II, and the FEA results in Section III, we can conclude that, for the case of deep-well motors (one pole pairs and an even number of rotor bars), there is always a set of PSHs that are not present in a perfectly symmetrical motor (e.g., PSHs(± 3) in the FEA section case, as well as in the field case of the next section). The amplitudes of these PSHs highly increase in the presence of an intern-turn short-circuit; moreover, these amplitudes show a strictly increasing trend with the severity of this fault.

If the supply is unbalanced or an eccentricity takes place, these PSHs amplitudes increase too (under rotor asymmetries, this effect does not take place, or is very light and only for high severity faults). To discriminate inter-turn short-circuits from these asymmetries, two more indexes must be obtained: VUI (increases only under voltage unbalance) and CUI (increases with intern-turn short-circuits, but does not increase under eccentricity and rotor faults. Moreover, it is also observed that the amplitudes of these PSHs behave differently when the inter-turn occurs. For instance, in the case analyzed, PSH(-3) with voltage unbalance shows a similar behavior than PSH(+3) with eccentricity and vice versa. Thus, their behavior also depends on the type of the second asymmetry. This might be due to the fact that they are associated to harmonic flux waves that rotate in different directions with different phases. Despite this, it has been shown that there is always one PSH that presents a strictly increasing behavior under stator fault. Therefore, a monitoring method using PSHs should always include two of the predicted harmonics in Section II, one associated to a clockwise rotating harmonic flux wave and the other a counter-clockwise one. Furthermore, it has also been observed that PSHs are reliable indicators in two of the line currents, therefore, only two of them need to be monitored, to assure that at least one of the PSHs amplitude obtained will present a strictly increasing trend under inter-turn short-circuit fault.

Taking into account all this information, three scenarios are possible if the amplitude of one or both of these PSHs increase: if the VUI increases, an unbalance supply problem is taking place; if the VUI is constant, and the CUI is constant too, an eccentricity failure (or a rotor asymmetry in very rare cases), might be taking place (this can be verified monitoring the amplitudes of the MEH and the LSH); if the VUI is constant and the CUI increases, then the increase of the amplitudes in these PSHs is due to an inter-turn short-circuit. This logic is reflected in Fig. 12 in the form of a continuous monitoring

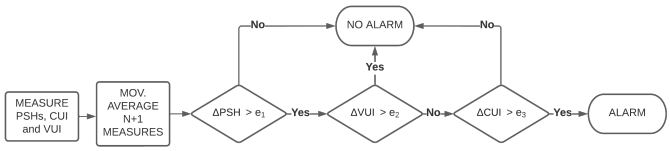

Fig. 12. Flux diagram of the proposed method.

diagnostic method. In order to account for error measurements and slight load variations (load is nearly perfectly constant in these applications), a moving average (taking $N+1$ samples), is applied to each indicator: PSHs, VUI and CUI; thresholds are used for each indicator: e_1, e_2 and e_3 (gathering data of machines with different powers is necessary to give precise values to these thresholds); finally the baseline values, from which the increments in the indicators are defined, are obtained by measuring the average values of the indicators during the initial period of monitoring and redefined when the thresholds are surpassed and the indicators stabilize again.

Finally, it should be remarked, that there could be a fourth scenario in which the VUI and PSHs increased simultaneously. In this case, it would not be possible to tell if what has occurred is a voltage unbalance or an inter-turn fault. Nevertheless, this is a very unlikely scenario, as it requires that both happen within the period between measure and measure. As the method is presented in the form of a continuous monitoring (several measures per day), the chances of this scenario to happen are very low. Furthermore, if the inter-turn fault was derived from the voltage unbalance, the voltages should be very high in order to breakdown the insulation. Yet, in this case, it is most likely that the over-voltage protection was triggered. Then, once the cause of the unbalance overvoltage was corrected and the motor put on normal operation (although with an inter-turn short-circuit), the alarms would be triggered since the proposed diagnostic scheme would have detected an increase in the PSHs, a non-increase in the VUI (it is corrected before a new measure), and another increase in the CUI.

V. Field case

A deep water well motor from a pumping station was continuously monitored for nearly a year, recording a steady-state of line currents and voltages every six operating hours. The motor is a Caprari M12230 (230 HP, p=1, 30 bars, 380 V Δ, 335 A, 2950 rpm), fed with a frequency converter at 43.97 Hz (model SD7058055 from Power Electronics) and operated at 70% of its rated current. The monitoring equipment consist of: three voltage probes, a three-phase current probe, a high-resolution oscilloscope, and a mini-PC (more details on the DAQ can be found in the Appendix A). Signals are sent via internet to a computer where the diagnostic algorithms are applied. The moving average takes 12 samples, and the thresholds for PSH (e_1), VUI (e_2) and CUI (e_3) are set, respectively, to 4 dB, 0.25 points and 0.25 points (details on how the thresholds are established are found in Appendix B).

Figures 13a, 13b, 13c, 13d and 13e show, respectively, the amplitude evolution over time (in dB with respect to the

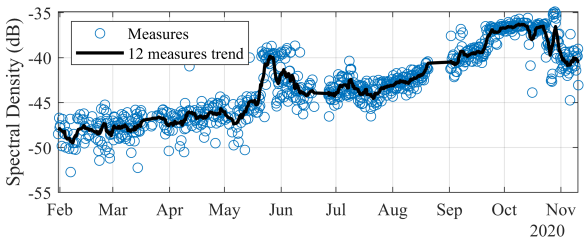

(a)

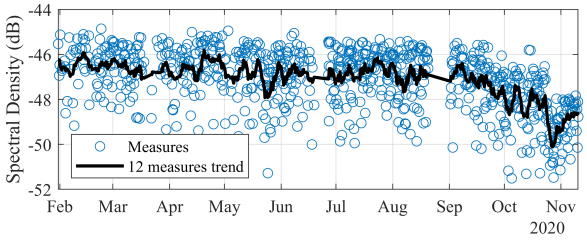

(b)

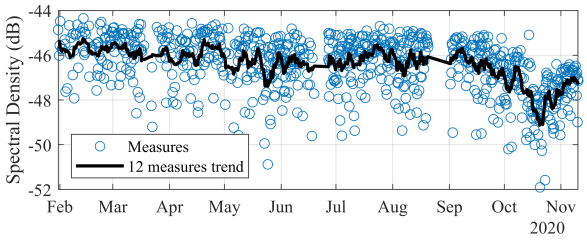

(c)

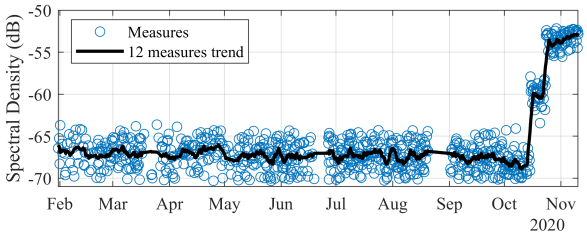

(d)

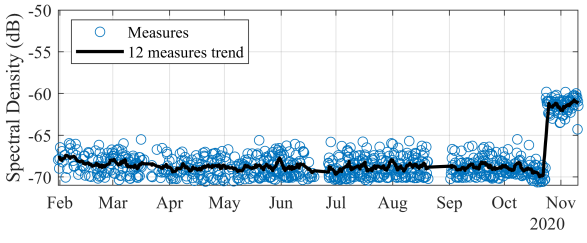

(e)

Fig. 13. Amplitude evolution over time of the LSH (a), the PSH(+1) (b), the PSH(-1) (c), the PSH(+3) (d) and the PSH(-3) (e).

fundamental component) of the LSH, the PSH(+1), the PSH(-1), the PSH(+3) and the PSH(-3) from line current A, while Figs. 14a and 14b show the evolution over time of the CUI and VUI.

As can be seen in Fig. 13a, there is a fault developing in the rotor from the very beginning (more details on the origin of this fault can be found in [3]). Despite this, PSHs and

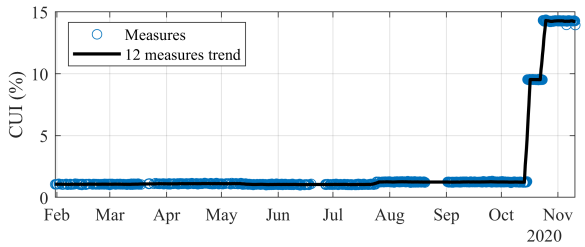

(a)

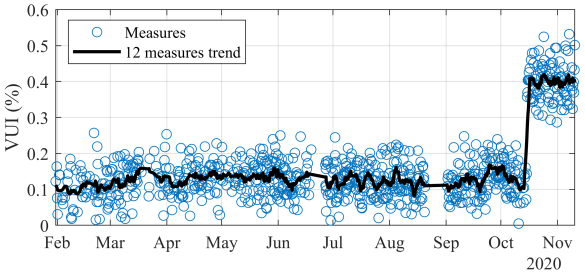

(b)

Fig. 14. Evolution over time of the CUI (a) and VUI (b).

CUI remain insensitive to the fault during the whole period, so no alarm is set for an inter-turn fault. On October 15, a simultaneous increase of 10 dB in the PSH(+3) and 8 points in the CUI, but also of 0.3 points in the VUI is detected, so no alarm is set. Seven days later, another simultaneous increase of 7 dB in the PSH(+3), 8 dB in the PSH(-3) and 5 points in the CUI is detected. Yet, in this case, the VUI does not increase, therefore, the alarm for inter-turn fault is triggered.

After two weeks from the last increase in the indicators, the motor was drawn from the deep-well (Fig. 15a) and sent to the motor repair shop for further inspection (Fig. 15b). There, it was found that the rotor end-rings were highly worn: this is a common fault in deep-well motors [3], explained in the introduction and detected here through the LSH amplitude increase shown in Fig. 13a. Regarding the stator fault, the repair shops of deep-well motors only apply simple tests to determine the state of the stator insulation: very conservative criterions are used, which easily imply rewind of the stator windings, to assure that the components will last longer when the motor is placed in a 100 to 500 m deep well, thus avoiding the high cost of extraction if an early fault takes place. First, the resistance between phases and ground is measured: if the result is under 200 MΩ, the stator is rewound. Second, the resistance between phases is measured to verify continuity. Visual inspection is used to look for a high amount of dirt, which in these motors it is also a reason to rewind. Looking for burn signs is not a standard procedure, and, moreover, it is not conclusive, since due to the small diameter of these motors, coil heads are placed in a very small space and cannot be thoroughly inspected, while the stator inside surface can just be partially seen (even a hand is hardly introduced in a 2 m long stator). Unfortunately, no surge test is applied. In the case of the motor monitored, no signs of burns were identified during the partial visual inspection, but the phase to ground resistance was below 200 MΩ, which confirmed the

(a) (b)

Fig. 15. Motor being removed (a) and sent for inspection (b).

stator damage, ordering its rewind, and validating the diagnosis made through the indicators proposed in the paper.

The field results are in total agreement with findings of previous sections. First, because the motor has two poles and 30 bars and the highest increases are observed in PSHs($\pm$3), just as predicted in Section II and verified in Section III. Second, because the PSHs and the CUI are insensitive to the rotor fault, thus agreeing with simulation results of Section III-C. Third, because the CUI behaves as expected and shows values in the same order of magnitude that the ones observed in Section III-A. Fourth, the PSHs($\pm$3) increase together with the VUI under an unbalanced voltage, and alone when the stator fault found in the motor repair shop takes place. Hence, since there are no load-oscillations, and no eccentricity is taking place, the PSHs increase can only be related to a stator fault.

Since the motor was able to continue operating after two weeks from the last change in the indicators, the results show that, in these motors, it is possible to detect the fault with this diagnostic scheme before it originates an unexpected shutdown, which in the case of the drinking water supply industry is a very sensitive issue. This means that the current flowing through the shorted turns was still too low to create a catastrophic failure. As proved in Table I, an incipient stator fault in this type of motors does not cause a destructive current (it can be even lower than rated current). Moreover, the double water cooling system prevents from a fast insulation degradation. It is not possible to give an accurate estimate of this current for this field case based only on the simulation results, since motors are of different sizes and operate at different speeds and loads. Nevertheless, everything (level of PSHs, CUI and no signs of burns) points in the direction of a short-circuit current not too high.

Finally, it is important to remark that these results are general and applicable to other models of deep-well induction motors since they present very similar characteristics to each other such as rotor construction, length proportionally higher than width and a small number of turns per slot. As for whether all conclusions could also be generalized for conventional induction motors, it is something that it is out of the scope in this study. However, what can be extrapolated for any type of PSHs producer induction motor is that there will always be a set of PSHs that are not present in the spectrum of the perfectly symmetrical healthy machine and will therefore always be more sensitive to the fault.

VI. Conclusion

This paper has analyzed in detail the use of PSHs as reliable indicators for early inter-turn fault detection in submersible inductions motors of deep-well pumps. The main findings and contributions of this work are listed below:

- Special characteristics of these machines make them suitable for inter-turn fault detection through PSHs, since they are highly water-cooled and they are normally designed with two poles and an even number of rotor bars.
- There is a set of PSHs that are highly sensitive to the fault, especially at early stages. These PSHs can be known beforehand, being only necessary to monitor two of them (one associated to a counter-clockwise rotating harmonic flux wave and the other to a clockwise), in two of the line currents.
- In the presence of other asymmetries, there is always one of these PSHs that maintains a monotonic behavior with the fault severity in one of the line currents.
- False positives due to voltage unbalance and eccentricity can be avoided if the line voltage and current unbalance indexes (VUI and CUI) are also monitored. Rotor cage faults cannot produce false positives.
- A novel diagnostic scheme has been proposed for reliable and early detection of inter-turn faults, which combines the monitoring of the PSHs and the line voltage and current unbalance indexes.
- Finally, and for the first time, the efficacy of a diagnostic scheme is proven by continuously monitoring a 230 HP industrial induction motor from a deep-well pump facility.

Appendix A: DAQ system

- PicoScope 4824A: High-resolution, deep-memory oscilloscope with 80 M/S sampling rate and 12 bits vertical resolution.
- PicoTech TA041: Active differential voltage probe with $\pm$ 2 % DC accuracy and 0 to 25 MHz frequency range.
- PicoTech TA325: 3-phase AC Rogowski current probe with $\pm$ 1 % of reading $\pm$ 0.1 A accuracy and 0.01 to 20 kHz frequency range.

Appendix B: Thresholds

To establish the thresholds of the fault indicators, data gathered from 10 deep-well motors continuously monitored during a year are analyzed. During healthy operation, VUI and CUI are relatively constant. For the field case in Section V: before any fault takes place, 0.04 and 0.13 points respectively are the maximum variations found with respect to the mean taken over 12 measures trend (black lines in Fig. 14). In the case of PSHs amplitudes, since the load is practically constant in this application, only small changes appear. For the field case: before any fault takes place, 1.6 dB for PSH(+3) and 1.32 dB for PSH(-3) are the maximum variations found with respect to the mean taken over the 12 measures trend (black lines in Fig. 13d and 13e). As observed next, the three thresholds

settled are higher than these maximum variations under healthy operation.

To establish the variations that should trigger an alarm, the FEA results are analyzed. With respect to the PSHs, it is observed in Fig. 6b that, for a low inherent VU (0.25% similar to that of the case of study), the PSH increases 5.3 dB from healthy to 1.52% shorted turns. Hence, PSH threshold should be a bit lower than this value to have a security margin: $e_1 = 4$ dB. With respect to VUI, it is also observed in this figure that an increase in the VUI from 0.25% to 0.5% (the minimum increase studied) originates an increase in the PSH of 6 dB when the motor is healthy and 3.5 dB for the lowest fault condition (1.52% shorted turns). The VUI threshold e_2 is set to 0.25 points. Finally, with respect to CUI, it is observed in Fig. 6c that, for a VUI $< 0.5\%$, the CUI increases 0.4 points from healthy to 1.52% of shorted turns. Hence, threshold should be a bit lower than this value to have a security margin: e_3 is set to 0.25 points.

Acknowledgment

We would like to thank FACSA for granting us access to their facilities.

References

[1] S. Jasechko and D. Perrone, "Global groundwater wells at risk of running dry," *Science*, vol. 372, no. 6540, pp. 418–421, 2021.

[2] M. J. Brandt, K. M. Johnson, A. J. Elphinston, and D. D. Ratnayaka, "Chapter 19 - pumping, electrical plant, control and instrumentation," in *Twort's Water Supply (Seventh Edition)*, seventh edition ed., pp. 777–828. Boston: Butterworth-Heinemann, 2017.

[3] J. Bonet-Jara, D. Morinigo-Sotelo, O. Duque-Perez, L. Serrano-Iribarnegaray, and J. Pons-Llinares, "End-ring wear in deep-well submersible motor pumps," *IEEE Trans. Ind. Appl.*, vol. 58, no. 4, pp. 4522–4531, 2022.

[4] H. Henao, C. Demian, and G.-A. Capolino, "A frequency-domain detection of stator winding faults in induction machines using an external flux sensor," *IEEE Trans. Ind. Appl.*, vol. 39, no. 5, pp. 1272–1279, 2003.

[5] G. N. Surya, Z. J. Khan, M. S. Ballal, and H. M. Suryawanshi, "A simplified frequency-domain detection of stator turn fault in squirrel-cage induction motors using an observer coil technique," *IEEE Trans. Ind. Electron.*, vol. 64, no. 2, pp. 1495–1506, 2017.

[6] M. Irhoumah, R. Pusca, E. Lefevre, D. Mercier, R. Romary, and C. Demian, "Information fusion with belief functions for detection of interturn short-circuit faults in electrical machines using external flux sensors," *IEEE Trans. Ind. Electron.*, vol. 65, no. 3, pp. 2642–2652, 2018.

[7] P. C. M. L. Filho, D. C. Santos, F. B. Batista, and L. M. R. Baccarini, "Axial stray flux sensor proposal for three-phase induction motor fault monitoring by means of orbital analysis," *IEEE Sensors J.*, vol. 20, no. 20, pp. 12 317–12 325, 2020.

[8] K. N. Gyftakis and A. J. M. Cardoso, "Reliable detection of stator interturn faults of very low severity level in induction motors," *IEEE Trans. Ind. Electron.*, vol. 68, no. 4, pp. 3475–3484, 2021.

[9] J. Seshadrinath, B. Singh, and B. K. Panigrahi, "Vibration analysis based interturn fault diagnosis in induction machines," *IEEE Trans. Ind. Informat.*, vol. 10, no. 1, pp. 340–350, 2014.

[10] P. Qin, Z. Zhang, Y. Sun, H. Liu, and H. Ren, "Vibration analysis of dfig stator winding inter-turn short circuit fault," in *2018 International Conference on Information Systems and Computer Aided Education (ICISCAE)*, pp. 436–442, 2018.

[11] P. S. Panigrahy and P. Chattopadhyay, "Tri-axial vibration based collective feature analysis for decent fault classification of vfd fed induction motor," *Measurement*, vol. 168, p. 108460, 2021.

[12] K. N. Gyftakis and J. C. Kappatou, "The zero-sequence current as a generalized diagnostic mean in δ-connected three-phase induction motors," *IEEE Trans. Energy Convers.*, vol. 29, no. 1, pp. 138–148, 2014.

[13] M. Singh and A. G. Shaik, "Incipient fault detection in stator windings of an induction motor using stockwell transform and svm," *IEEE Trans. Instrum. Meas.*, vol. 69, no. 12, pp. 9496–9504, 2020.

[14] D. Zheng, G. Lu, and P. Zhang, "A noninvasive interturn insulation condition monitoring method based on the common-mode impedance spectrum of inverter-fed machines," *IEEE Trans. Ind. Appl.*, vol. 57, no. 5, pp. 4786–4795, 2021.

[15] G. Joksimovic and J. Penman, "The detection of inter-turn short circuits in the stator windings of operating motors," *IEEE Trans. Ind. Electron.*, vol. 47, no. 5, pp. 1078–1084, 2000.

[16] A. Stavrou, H. Sedding, and J. Penman, "Current monitoring for detecting inter-turn short circuits in induction motors," *IEEE Trans. Energy Convers.*, vol. 16, no. 1, pp. 32–37, 2001.

[17] S. Cruz and A. Cardoso, "Diagnosis of stator inter-turn short circuits in dtc induction motor drives," *IEEE Trans. Ind. Appl.*, vol. 40, no. 5, pp. 1349–1360, 2004.

[18] M. Wolkiewicz, G. Tarchała, T. Orłowska-Kowalska, and C. T. Kowalski, "Online stator interturn short circuits monitoring in the dfoc induction-motor drive," *IEEE Trans. Ind. Electron.*, vol. 63, no. 4, pp. 2517–2528, 2016.

[19] M. Afshar, A. Tabesh, M. Ebrahimi, and S. A. Khajehoddin, "Stator short-circuit fault detection and location methods for brushless dfims using nested-loop rotor slot harmonics," *IEEE Trans. Power Electron.*, vol. 35, no. 8, pp. 8559–8568, 2020.

[20] M. Drif and A. J. M. Cardoso, "Stator fault diagnostics in squirrel cage three-phase induction motor drives using the instantaneous active and reactive power signature analyses," *IEEE Trans. Ind. Informat.*, vol. 10, no. 2, pp. 1348–1360, 2014.

[21] M. Bouzid and G. Champenois, "Experimental compensation of the negative sequence current for accurate stator fault detection in induction motors," in *IECON 2013 - 39th Annual Conference of the IEEE Industrial Electronics Society*, pp. 2804–2809, 2013.

[22] X. F. St-Onge, J. Cameron, S. Saleh, and E. J. Scheme, "A symmetrical component feature extraction method for fault detection in induction machines," *IEEE Trans. Ind. Electron.*, vol. 66, no. 9, pp. 7281–7289, 2019.

[23] F. Duan and R. Zivanovic, "Condition monitoring of an induction motor stator windings via global optimization based on the hyperbolic cross points," *IEEE Trans. Ind. Electron.*, vol. 62, no. 3, pp. 1826–1834, 2015.

[24] M. Sabouri, M. Ojaghi, J. Faiz, and A. J. Marques Cardoso, "Model-based unified technique for identifying severities of stator inter-turn and rotor broken bar faults in scims," *IET Electric Power Applications*, vol. 14, no. 2, pp. 204–211, 2020.

[25] I. Sahin and O. Keysan, "Model predictive controller utilized as an observer for inter-turn short circuit detection in induction motors," *IEEE Trans. Energy Convers.*, vol. 36, no. 2, pp. 1449–1458, 2021.

[26] G. H. Bazan, P. R. Scalassara, W. Endo, A. Goedtel, R. H. C. Palacios, and W. F. Godoy, "Stator short-circuit diagnosis in induction motors using mutual information and intelligent systems," *IEEE Trans. Ind. Electron.*, vol. 66, no. 4, pp. 3237–3246, 2019.

[27] S. Nandi, S. Ahmed, H. Toliyat, and R. Bharadwaj, "Selection criteria of induction machines for speed-sensorless drive applications," *IEEE Trans. Ind. Appl.*, vol. 39, no. 3, pp. 704–712, 2003.

[28] P. Vas, *Parameter Estimation, Condition Monitoring, and Diagnosis of Electrical Machines*, ser. Monographs in Electrical and Electronic Engineering: 27. Clarendon Press, 1993.

[29] K. N. Gyftakis, "A comparative investigation of interturn faults in induction motors suggesting a novel transient diagnostic method based on the goerges phenomenon," *IEEE Trans. Ind. Appl.*, vol. 58, no. 1, pp. 304–313, 2022.

[30] W. Thomson and A. Barbour, "On-line current monitoring and application of a finite element method to predict the level of static airgap eccentricity in three-phase induction motors," *IEEE Trans. Energy Convers.*, vol. 13, no. 4, pp. 347–357, 1998.

[31] S. B. Lee, D. Hyun, T.-j. Kang, C. Yang, S. Shin, H. Kim, S. Park, T.-S. Kong, and H.-D. Kim, "Identification of false rotor fault indications produced by online mcsa for medium-voltage induction machines," *IEEE Trans. Ind. Appl.*, vol. 52, no. 1, pp. 729–739, 2016.

Jorge Bonet-Jara received the B.Sc degree in Industrial Engineering and the Master in Electrical Engineering from the Universitat Politècnica de València (UPV, Spain), in 2016 and 2018, respectively.

He is currently conducting his Ph.D in Fault Diagnosis and Sensorless Speed Estimation in the Electric Engineering Department of the UPV. His research interests include condition monitoring and modelling of electrical machines.

Joan Pons-Llinares (M'13) received the M.Sc. degree in Industrial Engineering and the Ph.D. degree in Electrical Engineering from the Universitat Politècnica de València (UPV, Spain), in 2007 and 2013, respectively.

He is currently an Associate Professor at the Electric Engineering Department of the UPV. His research interests include time-frequency transforms, condition monitoring and efficiency estimation of electrical machines.

Konstantinos N. Gyftakis (M'11, SM'20) received the Diploma in Electrical and Computer Engineering from the University of Patras, Patras, Greece in 2010. He pursued a Ph.D. in the same institution in the area of electrical machines condition monitoring and fault diagnosis (2010-2014). Furthermore, he worked as a Post-Doctoral Research Assistant in the Dept. of Engineering Science, University of Oxford, UK (2014-2015). Then he worked as Lecturer (2015-2018) and Senior Lecturer (2018-2019) in Coventry University, UK. Between 2015-2022 he worked as a Lecturer in Electrical Machines, University of Edinburgh.

He is currently an Associate Professor with the Technical University of Crete, Greece. His research interests focus in the fault diagnosis, condition monitoring and degradation of electrical machines. He has authored more than 120 papers in international scientific journals and conferences and chapter for the book: "Diagnosis and Fault Tolerance of Electrical Machines, Power Electronics and Drives", IET, 2018. Finally he serves as an Associate Editor for the IEEE Transactions on Energy Conversion and the IEEE Transactions on Industry Applications.